



ALMA EOC Polarization Commissioning

P. C. Cortes^{1,2}, S. Kamen^{1,3}, K. Nakanishi³, C. Hull^{2,7}, G. Moellenbrock², E. Fomalon², E. Humphries⁴, W. D. Cotton², R. Paladino^{5,8}, H. Nagai³, J. M. Girart⁶, C. Brogan², A. Remijan².

1. ALMA/JAO
2. NRAO
3. NAOJ
4. ESO
5. INAF-ORA
6. CSIC-IEEC
7. Harvard/CFA
8. University of Bologna

Introduction

As the premier instrument in the millimeter and sub-millimeter wavelengths, ALMA also offers polarization capabilities. For the current cycle (cycle-3), ALMA is offering:

- Continuum linear polarization.
- Arbitrary frequencies in TDM mode with single spectral windows per baseband and 64 channels per polarization product (XX, YY, XY, and YX).

As part of the Extension and Optimization of Capabilities (EOC), we are working on advancing the following ALMA polarization aspects:

- Spectral-Line polarization at arbitrary frequencies and spectral resolutions
- Increasing the field of view to the FWHM of the primary beam

The final set of capabilities will be announced at the call for proposals.

Continuum linear polarization

The ALMA continuum polarization capabilities have been offered since cycle 2. The mode is offered with 64 channels per polarization product, with one spectral window (with an effective bandwidth of 1.75 GHz) per baseband. The ALMA continuum polarization have been demonstrated using the well known VLA calibrators 3c286 and 3c138 (where [1] shows the VLA maps of 3c286 at 1.4, 4, and 8 GHz). The ALMA science verification observations were done in band 6 using *session* mode and the ALMA online query software (with the exception of the polarization calibrator). The data was calibrated and imaged using casa (see 3c286 online casaguide [2]). Figure 2 shows the ALMA band 6 continuum image for 3c286.

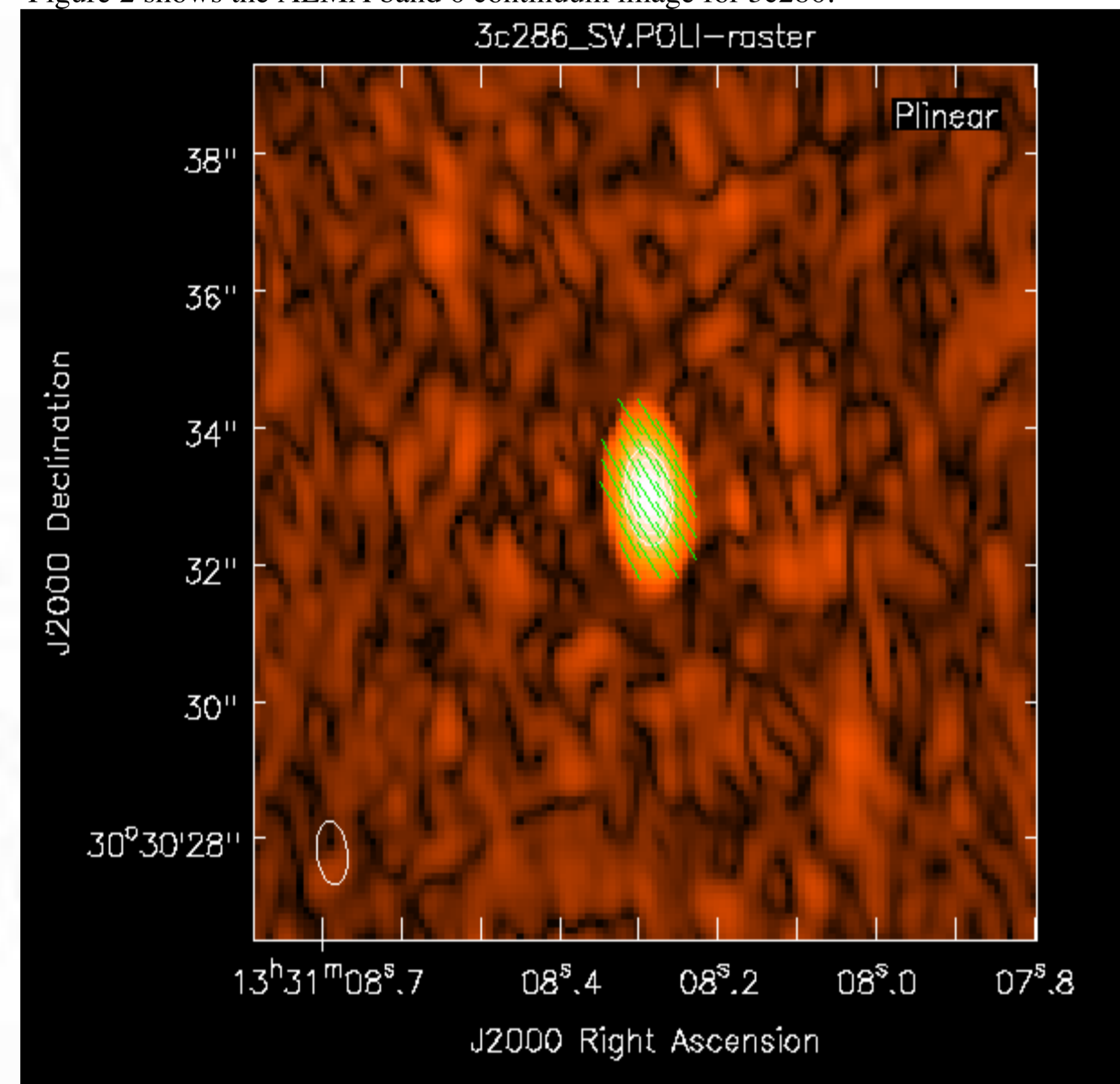


Figure 1. Here the ALMA band 6 continuum linear polarization is shown. The Stokes I is presented as color scale and the normalized linear segment map is shown in green.

Parameter	Value	Error
I [mJy]	375.6	0.35
Q [mJy]	14.4	0.04
U [mJy]	60.1	0.09
P [mJy]	61.8	0.05
F [%]	16.45	0.02
χ [°]	38.2	0.02

Table 1. ALMA 3c286 science verification main results.

The ALMA results agree very well with the literature having an EVPA of 38.2 ± 0.02 and polarized intensity of 16.8 mJy. The detailed results are listed in Table 1. IRAM 30 m Telescope observations presented results of single-dish millimeter measurements of 3C286 [3]. Their observations at 1 mm (229 GHz) and 3 mm (86 GHz) produced similar results to ours, later confirmed by CARMA polarization observations taken at 1 mm (225 GHz) [4,5]. These results are summarized in Table 2. Now, the uncertainties quoted in Table 1 are purely statistical. The systematic errors will be larger, and include (but are not limited to) any net bias in the position angle of the linear feeds in the antennas, the details of different observations (at what parallactic angles, etc.), and other data quality variations (including source structure). We conservatively estimate the position angle uncertainty to be $\pm 2^\circ$.

Parameter	1 mm	3 mm
$F_{\text{IRAM}}[\%]$	14.4 ± 1.8	13.5 ± 0.3
$\chi_{\text{IRAM}}[^\circ]$	33.1 ± 5.7	37.3 ± 0.8
$\chi_{\text{CARMA}}[^\circ]$	39.2 ± 1.0	-

Table 2. The IRAM results at 1 and 3 mm [3] are listed in rows 1 and 2. The CARMA results at 1 mm are listed in row 3 [4,5] (only the EVPA was available).

ALMA cycle-2 has finalized and a significant number of polarization projects have been executed. Although still in *best efforts*, the improvements in the online software stability will allow us to increase our efficiency in cycle-3.

Spectral-line linear polarization

We have conducted commissioning of the linear polarization capabilities with ALMA in frequency space. The evolved star IK-Tau, which has been mapped in linear polarization by [6] in both SiO(5-4) and CO(2-1) thermal linear polarization emission (Golreich-Kylafis effect) with the SMA, was used as target. We studied the instrumental polarization properties as a function of spectral resolution and reproduced the SMA results on this source. The Figure 3 shows the instrumental polarization solutions (D-terms) of a representative antenna (DV22) in band 3. The spectral shape of the D-term solution is smooth, uniform and no spur like structure is seen even in highest frequency resolution mode. The difference in amplitude is due to the different signal to noise requirements at different spectral resolutions (these solutions have been determined from data taken simultaneously at different channel resolutions). This demonstrates that the instrumental polarization is mostly spectral resolution independent for these datasets.

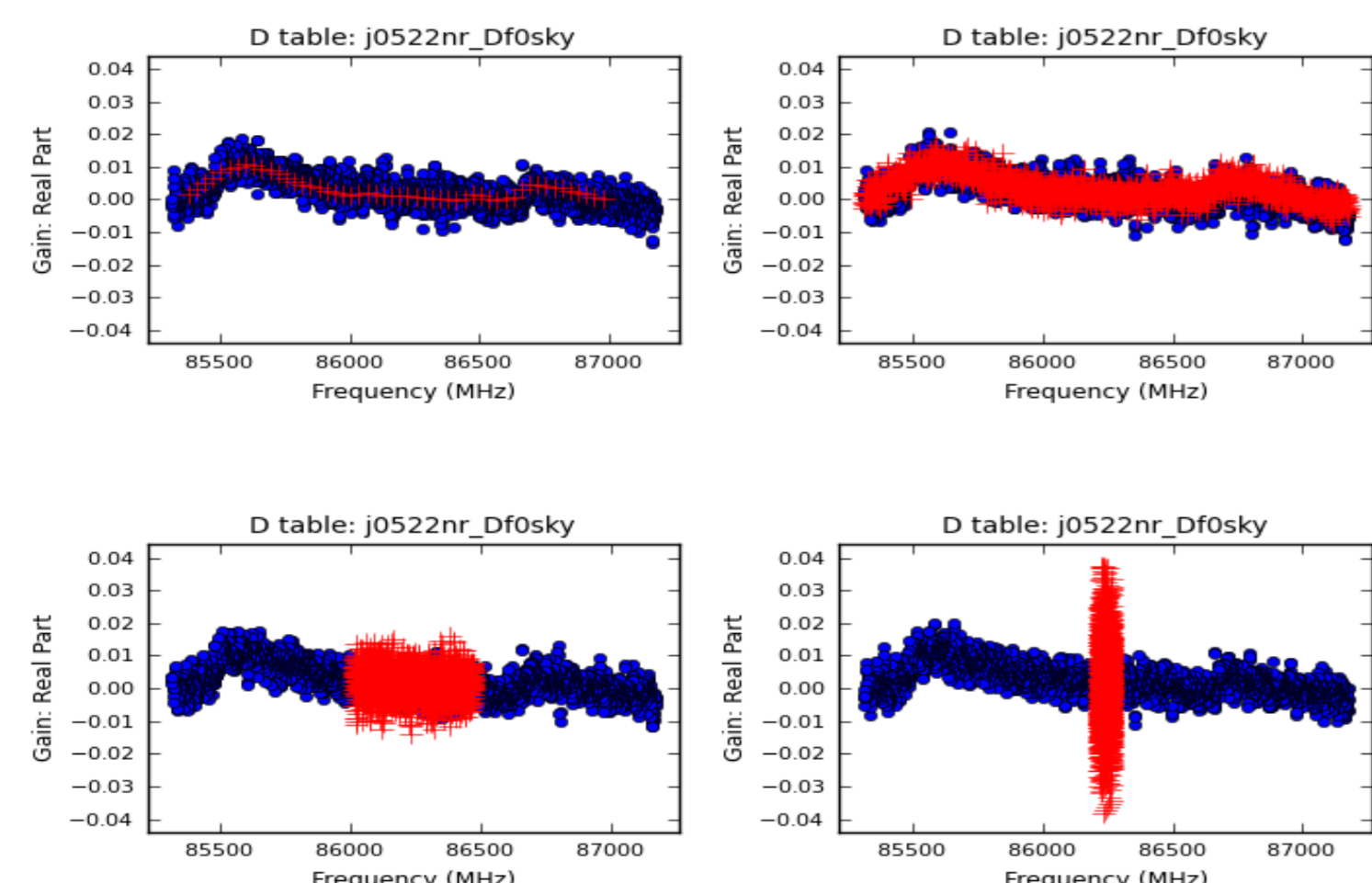


Figure 2. D-term plot for a representative antenna (DV22). Blue circles and red crosses show the D-term obtained with FDM, 0.9 MHz, 244, and 30.5 KHz channel resolution respectively.

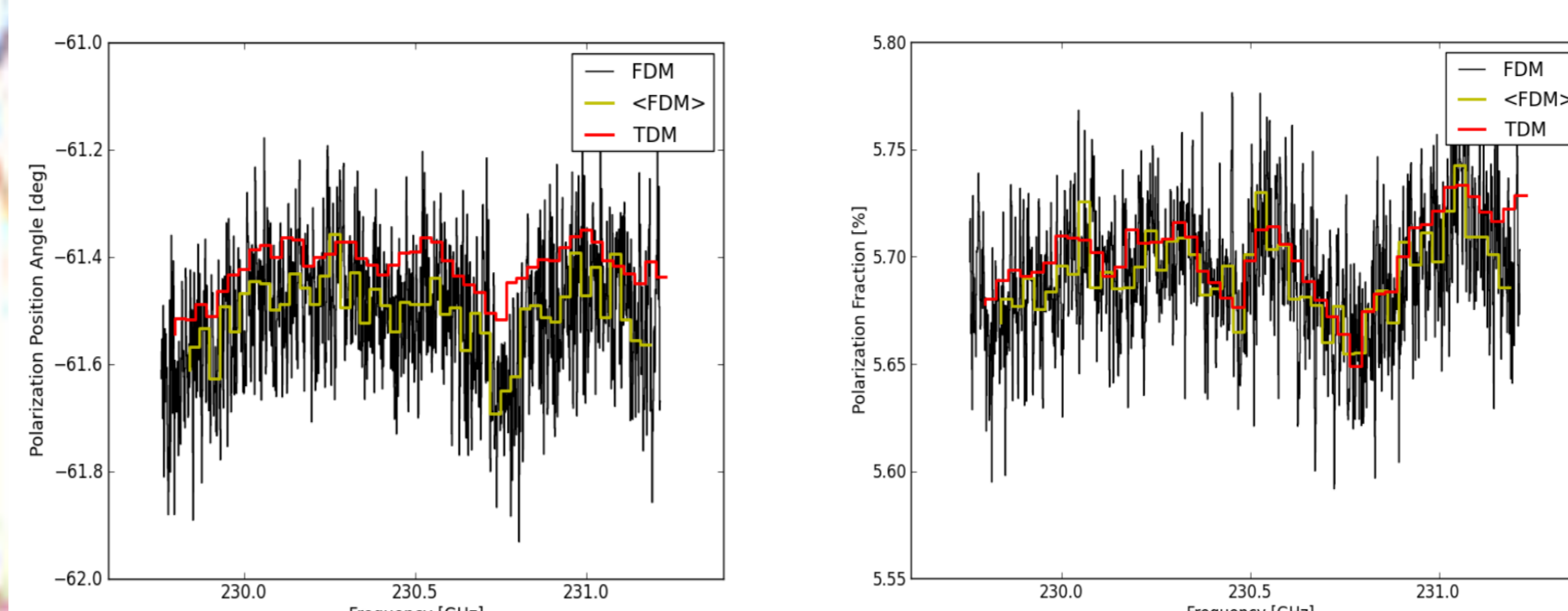


Figure 3. (Right) The polarization position angle from the TDM (red), FDM (black), and averaged 64 channels FDM (yellow) for the J0522-364 calibrator is shown here. (Left) The fractional polarization as shown previously, same color code applies.

From Figure 3 we see that both the fractional polarization and the EVPA between the FDM 2 GHz and the TDM spectral windows agree well within 0.09 degrees in the mean (or about 0.1 %). The fractional polarization is also displayed in Figure 3. Here we also see very good agreement between the TDM and FDM 2 GHz spectral windows with a stable fractional polarization spectrum around a mean value of 5.69% for the calibrator.

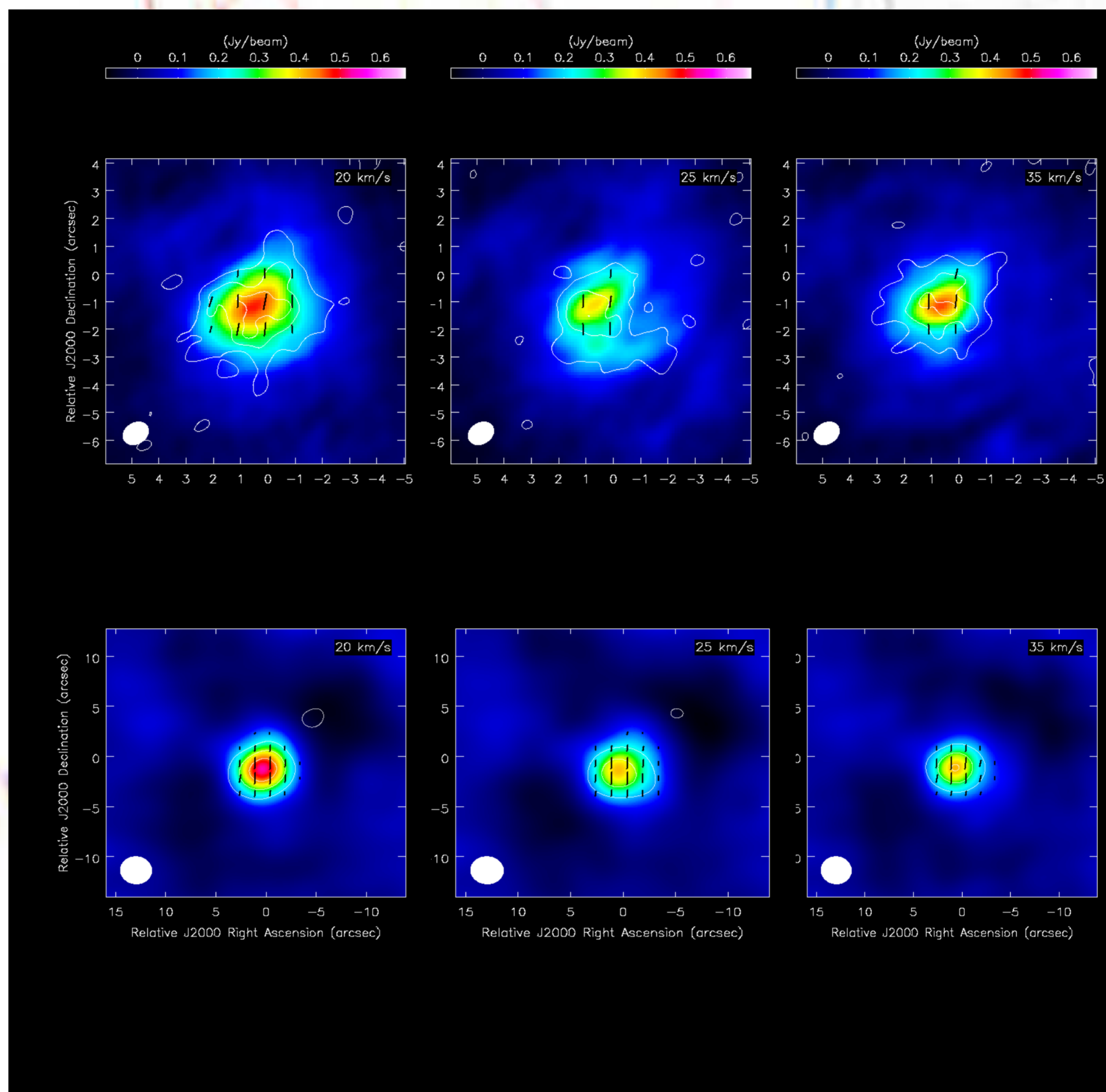


Figure 4. ALMA native channel maps (upper panel) and the ALMA smoothed data (lower panel). Note that the beam is also shown as a white filled ellipse. The Stokes I emission is shown as color scale, the Rician debiased polarized intensity is shown in contours of 3.5, 7.1, 10.7, and 14.2 mJy/beam for the native resolution data, and 20, 40, 60, and 80 mJy/beam for the smoothed data. The position angle and fractional polarization are shown as black line-segments.

The SMA results on IK Tau reported polarized emission only at channels 20, 25, and 35 km/s, where their EVPA are predominantly oriented north-south with values ranging from -10 to 10 degrees. Figure 4 shows our results for IK Tau CO(2-1) polarized emission. The Stokes I image is superposed with the Rician debiased polarized intensity in contours, and the polarization line-segment maps. The Figure also shows the ALMA data convolved with the SMA beam. The Figure 5 shows the histograms of EVPA and fractional polarization from our data. The range of position angles in our channels goes from -10 to 0 degrees with a small tail reaching up to +10 degrees, which is in well agreement with [6] results. However, the fractional polarization reported by [6] is as large as 13%, which we do not reproduce. Nevertheless, the ALMA values agree with predictions from [7] about CO(2-1) expected fractional polarization.

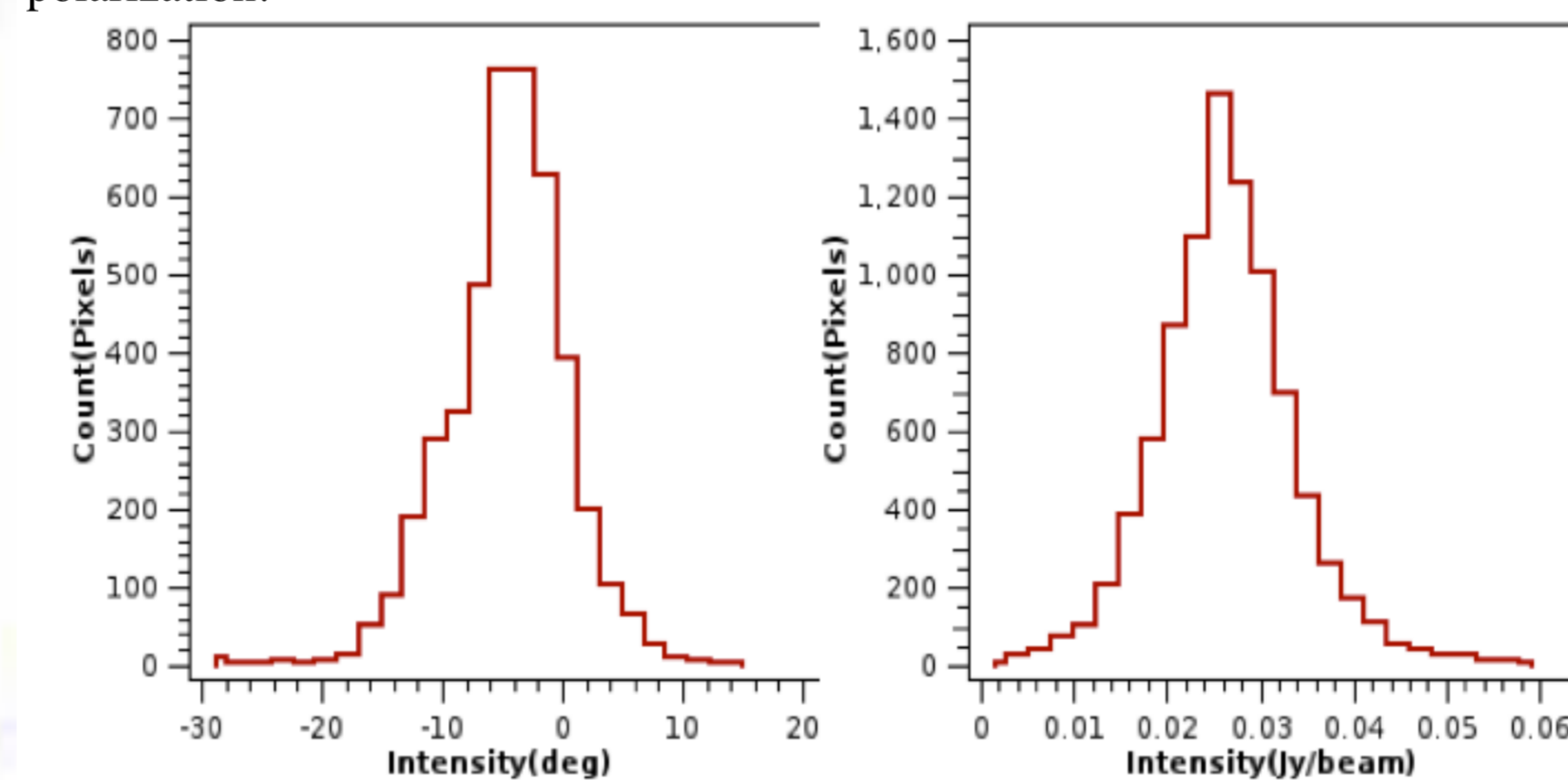


Figure 5. (Left) The distribution of EVPA in our data is shown. (Right) The fractional polarization histogram is shown with a peak distribution about 3%. The labels in the x axis do not corresponds to the actual data due to a bug in the CASA viewer.

Wide-field linear polarization

The ALMA System Technical Requirements defines the *off-axis* cross polarization requirement as:

1. For the antenna plus front-end, the cross-polarization shall be < -20 dB before calibration, but after the *on-axis* cross polarization has been subtracted. This applies to the -6 dB contour of the primary beam.
2. Assuming a 10% calibration accuracy, this allows a cross-polarization of < -34 dB after calibration and after the *on-axis* cross-polarization has been removed.

The cycle-2 polarization commissioning campaign showed that some antennas violated requirement (1) with D-term levels of about 15% at -3 dB beam, which limited the FoV to 1/3 FWHM. For the EOC campaign, we are attempting to characterize the polarization properties within a wider FoV of -6 dB contour of the primary beam ($\sqrt{2} \times$ FWHM) using the astro-holography technique on 3c279 using band 3 in continuum and custom mosaics of 11x11 points done in the antenna frame. Figure 6 shows a description of the astro-holography technique. The Figure 7 shows the histogram for the *on-axis* D-terms. The values are well within the specification.

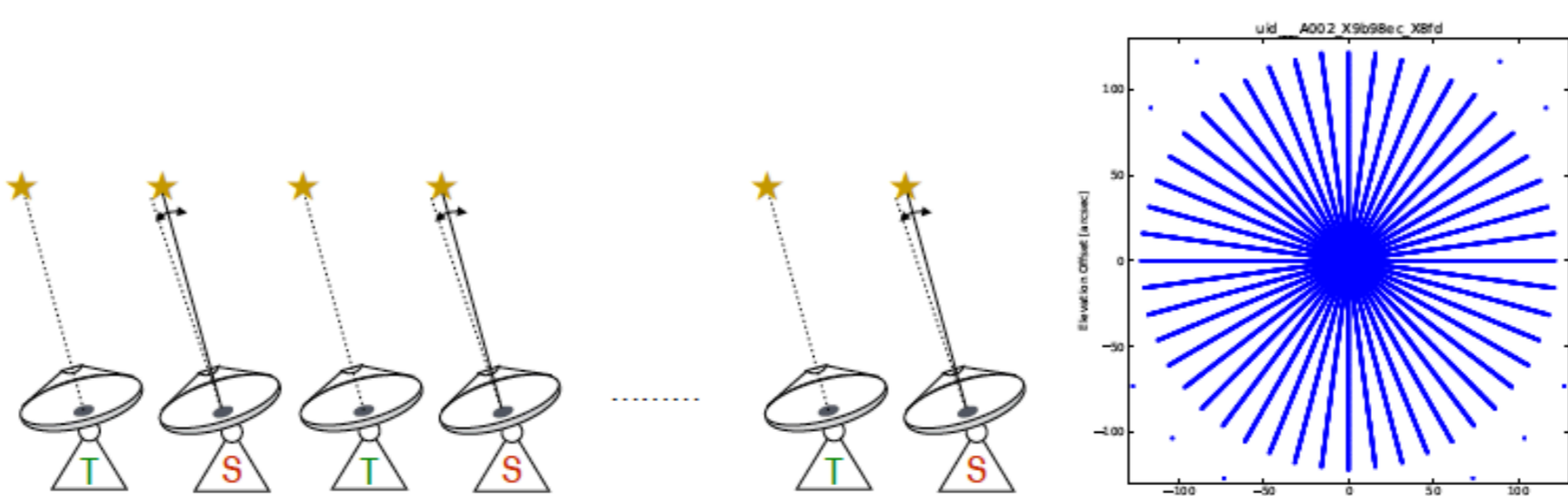


Figure 6. The array is separated into two groups: tracking (T) and scanning (S). While the T antennas point to the target source *on-axis*, the S antennas scans a radial pattern centered in the source with 24 excursions to cover the *off-axis* points within the field of view.

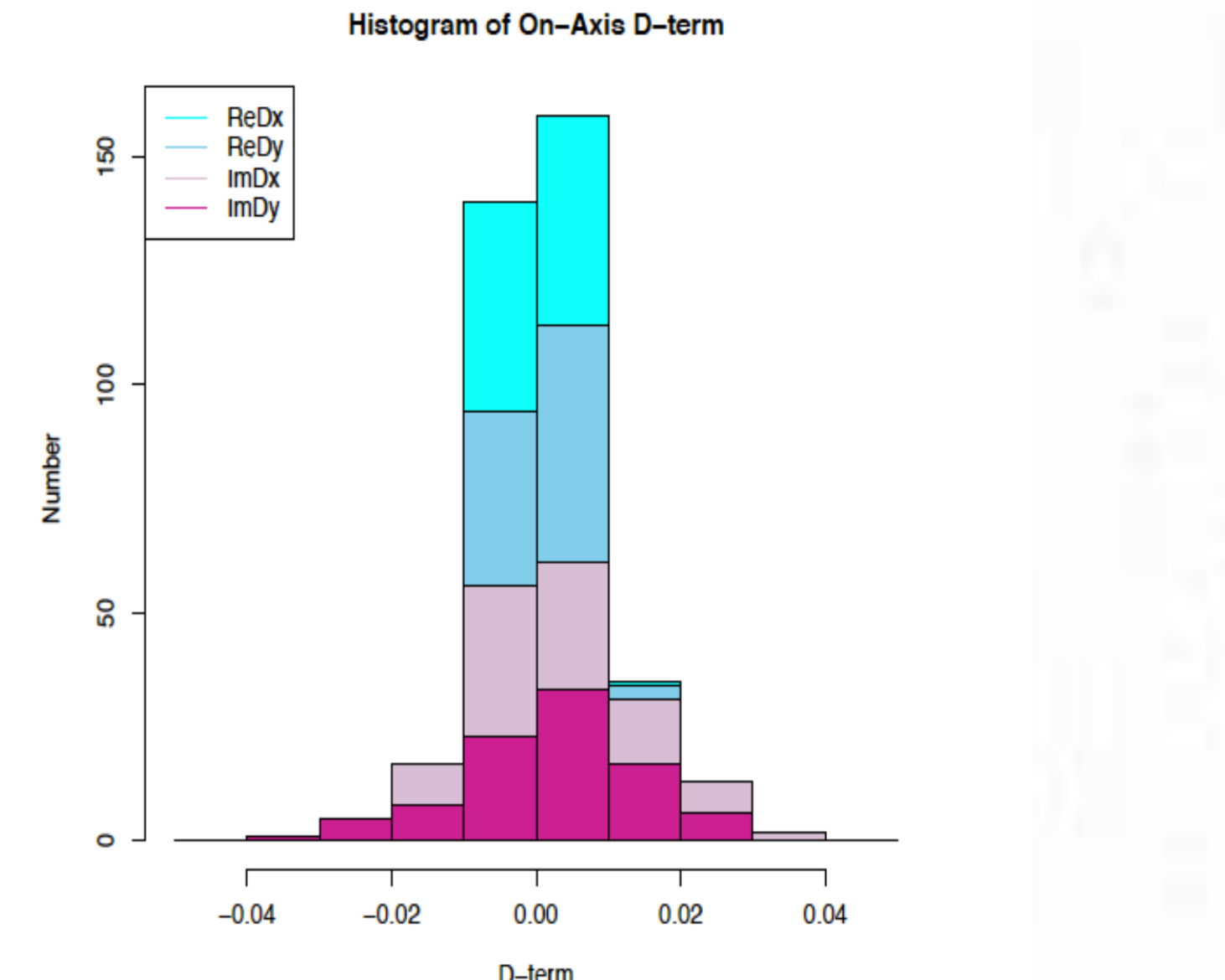


Figure 7. Histogram of the on-axis D-term values. The colors of cyan, sky blue, thistle, and violet stand for ReD_x , ReD_y , ImD_x , and ImD_y .

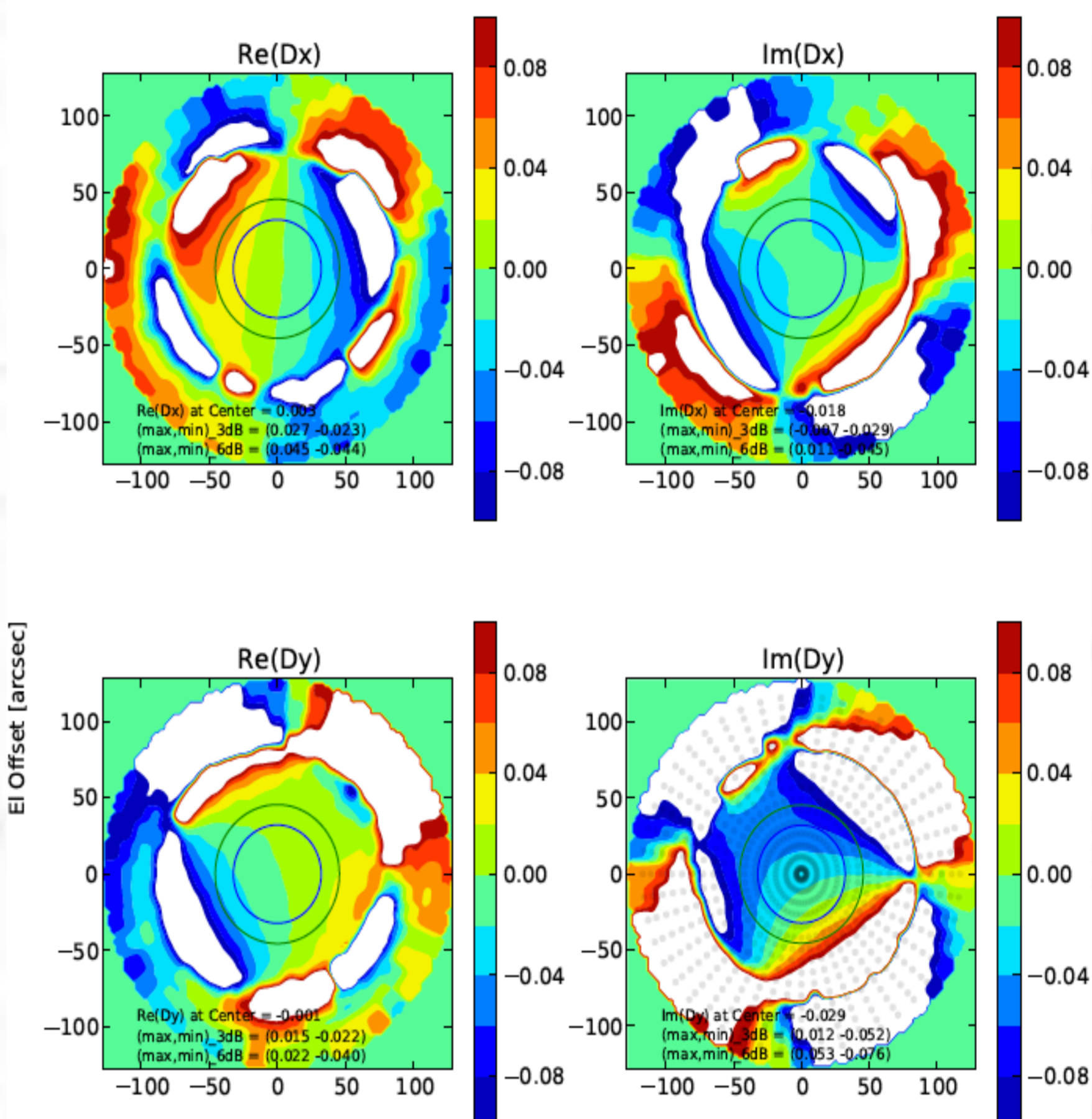


Figure 8. D-term distribution for DA41 (top panel) from astro-holography measurements. Blue and green circles indicate the beam-width at -3 dB and -6 dB with respect to the beam center. The gray dots in the ImD_y map indicate sampling points. The color indicator ranges ± 0.1 and white area stands for where $|D| > 0.1$, and derived error maps for Q, U, and F from the 11x11 custom mosaic (bottom panel). The outer dotted line is the FWHM of the primary beam; the inner dotted line is 1/3 of the FWHM (the continuum linear polarization restriction in Cycles 2 and 3). In all cases the central value has been subtracted from all of the off-axis pixels. The contours trace out different levels of the residuals in the maps. Each pixel of the Q and U error maps was first normalized by dividing by the Stokes I value in the corresponding pixel.

From the astro-holography analysis, D-terms were calculated for each point in the scanning pattern. The D-term distribution showed median values of 0.03 and 0.05 for beam areas of -3 dB and -6 dB, respectively, while the D-term values at the beam center were 0.0049 (less than 1%). The D-term-corrected polarization measurements resulted in < 0.37% and < 0.75% departures from Stokes Q, U, and V within the beam areas of -3 dB and -6 dB, compared from the *on-axis* Stokes parameters. The -3 dB marks the $1/2 \times$ FWHM beam area and -6 dB the $\sqrt{2} \times$ FWHM level, which is important for mosaics (results are shown in Figure 8, upper panel for DA41). The 11x11 custom mosaic observations (also on 3c279), also mapped the primary beam but using a regular rectangular scanning pattern and only applying an *on-axis* D-term correction. The main results here are as follows: (1) After *on-axis* calibration of all offset pointings in all bands, and within the FWHM of the primary beam, the error in polarization fraction $F_{\text{frac, err}} = F_{\text{frac, on}} - F_{\text{frac, off}} < 0.01$. The error in the EVPA $\chi_{\text{err}} = \chi_{\text{on}} - \chi_{\text{off}} < 4$ degrees. (2) For all bands, all offset pointings, and all antennas, the *off-axis* leakage amplitudes are $|D| < 0.1$ (for the astro-holography data, some antennas show large than 0.1 deviations *off-axis*). (3) The differences in the error maps are negligible for the two types of antennas (DA and DV) present in the datasets (results are shown in Figure 8, lower panel). The results obtained by both test are consistent between each other, though, astro-holography produced slightly better error maps. The next step in our investigation is to use these results to produce detail error maps that the community can use to interpret the *off-axis* polarization results.

References

- [1] Aklujar, C. E., Garrington, S. T., 1995, A&AS, 112, 235
- [2] 3c286 casaguide – <https://casaguides.nrao.edu>
- [3] Agudo, I. et al. 2012, A&A, 541A, 111
- [4] Hull, C. L.H, Plambeck, R. L., 2015, JAI, 4, 1n02, 1550005
- [5] CARMA Memo 64
- [6] Vlemmings et al., 2012, A&A, 540L, 3
- [7] Cortes, P. C., Crutcher, R. M., Watson, W. D., 2005, ApJ, 628, 780